Quaternary Research 77 (2012) 433–444

Contents lists available at SciVerse ScienceDirect

Quaternary Research

journal homepage: www.elsevier.com/locate/yqres

Organic stable carbon isotopic composition reveals late Quaternary vegetation changes in the dune fields of northern China

Huayu Lu [a,b,*], Yali Zhou [c], Weiguo Liu [d], Joseph Mason [b]

[a] School of Geographic and Oceanographic Sciences, the MOE Key Laboratory of Coast and Island Development, Nanjing University, Nanjing 210093, China
[b] Department of Geography, University of Wisconsin Madison, WI 53706, USA
[c] College of Tourism and Environment, Shaanxi Normal University, Xian 710062, China
[d] Institute of Earth Environment, State Key Laboratory of Loess and Quaternary Geology, Chinese Academy of Sciences, Xian 710075, China

ARTICLE INFO

Article history:
Received 3 February 2011
Available online 17 February 2012

Keywords:
Dune fields
Stable carbon isotopes
C_4 plants
Vegetation changes
Climatic change
Northern China
Late Quaternary

ABSTRACT

Vegetation changes during the late Quaternary in the dune fields of northern China are not well understood. We investigated organic carbon stable isotopic composition of surface soils, related mainly to the ratio of C_3 and C_4 plants, across a range of arid to subhumid climates in this region. Isotopic composition is weakly related to both temperature and moisture (multiple $R^2 = 0.53$), with the highest $\delta^{13}C$ (greatest C_4 abundance) in the warm, subhumid Horqin dune field. In late Quaternary, eolian stratigraphic sections of the Mu Us and Horqin dune fields, but not in the much colder Otindag dune field, $\delta^{13}C$ is higher in organic carbon from paleosols than in eolian sands. This contrast, most evident for paleosols recording a major early to middle Holocene phase of dune stabilization, is interpreted as evidence for expansion of C_4 plants due to increased effective moisture, high temperature because of high insolation, and decreased disturbance related to eolian erosion and deposition.

1. Introduction

Dune fields are scattered discontinuously along the Gobi desert belt in central and eastern Asia, covering a total area of around 400,000 km^2, with annual precipitation ranging from 150 to 500 mm and mean annual temperatures between 2 and 9°C. The dune fields form an important part of a major dust source region, with local to global environmental impacts, and vegetation plays a vital and direct role in modulating dust emission (Zhang et al., 2003; Wang et al., 2006; Zhang et al., 2008; Maher et al., 2010). Vegetation in the dune fields and surrounding drylands is sensitive to climatic changes which may be related to both the precipitation brought by the Asian monsoon circulation and local insolation (temperature) (Lv et al., 2002; Wang, 2006; Xu et al., 2009; Rao et al., 2010; Lu et al., 2011). Therefore, a better understanding of vegetation changes in the dune fields would be very helpful in understanding local and regional environmental changes and even global impacts of the dust from Asia, such as possible effects on primary productivity in oceans and atmospheric CO_2 (Martin and Fitzwater, 1988; Maher et al., 2010). Some researchers also suggest that over-grazing by domestic livestock has damaged the vegetation cover resulting in frequent dust emission and strengthened desertification (Sun, 2000; Wu and Ci, 2001; Wang, 2008). Separating the influences of climatic change and human disturbance on vegetation change is still an open question, which can be addressed in part by studying vegetation response to climatic change before the time of major human impacts.

Previous investigations in these dune field regions have advanced our understanding of variations in environmental conditions and vegetation composition, in particular during the late Pleistocene and Holocene (Dong, 2002; Xiao et al., 2002, 2004; Huang et al., 2005; Sun et al., 2006; Wang et al., 2009; Wen et al., 2010; Zhai et al., 2011). However, there are still several fundamental issues to be resolved in order to obtain a reliable vegetation record. One is that the previous data come from studies of a small number of widely scattered lakes or wetlands; it is not clear whether these records adequately represent vegetation change in the dune fields. The second problem is that independent age control was limited in previous studies; most records of environmental change extracted from lacustrine or eolian sediments were supported by only a few separate radiocarbon or optically stimulated luminescence (OSL) ages (e.g., He et al., 2010; Yang et al., 2010). Because of the great temporal and spatial variability of eolian sand/silt sedimentation rates in dune field environments, depositional hiatuses and erosional unconformities are present and sediment ages cannot be accurately interpolated between sparse radiocarbon or OSL samples. A third problem is that pollen is not well preserved in coarse-grained deposits and alkaline environments (Li et al., 2003). Thus, it is essential to develop new sources of information on past vegetation change in these dune fields.

* Corresponding author at: School of Geographic and Oceanographic Sciences, the MOE Key Laboratory of Coast and Island Development, Nanjing University, Nanjing 210093, China.
E-mail address: huayulu@nju.edu.cn (H. Lu).

0033-5894/$ – see front matter © 2012 University of Washington. Published by Elsevier Inc. All rights reserved.
doi:10.1016/j.yqres.2012.01.009

Stable carbon isotopic composition of soil organic matter ($\delta^{13}C$) has been widely used to reconstruct changes over time in the relative proportions of plants using C_3 and C_4 photosynthetic pathways, based on differences in discrimination against ^{13}C that occurs when atmospheric CO_2 is fixed by these two pathways (Cerling, 1984; O'Leary, 1988; Cerling et al., 1989; Quade et al., 1989, 1995; Ehleringer and Cerling, 2002). The $\delta^{13}C$ values of C_3 plants range globally from −20 to −32‰, averaging around −27.0‰; while C_4 plants have $\delta^{13}C$ values between −10 and −17‰, with a mean of −14.0‰ (Ode et al., 1980; Farquhar et al., 1989; Liu et al., 2005a,b). When plant-derived organic carbon is added to soils and sediments, this large contrast in $\delta^{13}C$ is preserved, despite minor additional fractionation when plant material is decomposed in soils and sediments (Melillo et al., 1989; Quade et al., 1989, 1995; Wedin et al., 1995; Connin, 2001; Wiesenberg et al., 2004).

In eolian sediments, organic carbon isotope analyses can often be interpreted using isotopic data from modern surface soils and associated natural vegetation as analogs. For example, this approach has provided valuable new insight on late Quaternary vegetation change in the U.S. Great Plains (Fredlund and Tieszen, 1997; Feggestad et al., 2004; Johnson et al., 2007; Nordt et al., 2008). In the Chinese Loess Plateau, there have been several studies of C_3/C_4 changes revealed by organic carbon isotopes (Gu et al., 2003; Zhang et al., 2003; Vidic and Montañez, 2004; An et al., 2005; Liu et al., 2005a,b; Liu and Huang, 2008; Rao et al., 2010), showing that the proportion of C_4 plants increases with higher temperature and precipitation. This result is consistent with research in other regions indicating that precipitation as well as temperature influence the mixture of C_3 and C_4 plants in many ecosystems (e.g., Hattersley, 1983). These conclusions can be complemented by the results of inorganic carbon isotope analyses using pedogenic carbonates in the southern Chinese Loess Plateau (Wang et al., 1997; Wang and Follmer, 1998). However, detailed reconstruction of late Quaternary vegetation change in the dune fields and deserts north of the Chinese Loess Plateau has not been undertaken.

In this study, eolian sediments and buried soils formed in them were sampled for stable isotope analysis of organic carbon in three dune fields of northern China. Modern surface soil samples from dune fields and deserts of the same region were sampled to study relationships between climate and $\delta^{13}C$ of organic matter. Variation of the organic carbon isotopic composition in paleosols and eolian sediments is interpreted as the result of change in the relative abundance of C_3 and C_4 plants over time. These inferred vegetation changes are related to climatically driven change in dune field stability, as interpreted independently from stratigraphic evidence. This is the first use of stable carbon isotopes in organic matter from soils and sediments as an indicator of vegetation history in the dune fields and deserts of northern China.

2. Setting and sampling

Stratigraphic profiles containing eolian sediments and soils were sampled in three dune fields. The Mu Us dune field (Fig. 1) has an area of ~50,000 km^2 with a mean annual temperature (MAT) of 8.2°C, and mean annual precipitation (MAP) of 349 mm, in which 60–70% of the rain falls in June, July, and August. The higher plant flora of at least 1106 species includes members of 98 families and 420 genera. The most abundant species are *Artemisia ordosica*, *Psammochloa villosa* (a C_4 grass), *Pycnostelma lateriflorum*, *Salix cheilophila*, *Salix microstachya* in the Mu Us dune field (Li et al., 2005), and the abundance of C_4 plants increases significantly with precipitation (Yin and Li, 1997).

The Otindag dune field (Fig. 1) has an area of ~30,000 km^2 with a MAT of 2.5°C and MAP of 266 mm (this is our new estimate; Liu and Wang (2005) reported 2.2°C and 288 mm, respectively). The vegetation is grassland with shrubs and scattered trees, with over 60% of the species of modern plants using the C_3 photosynthesis pathway. Plants

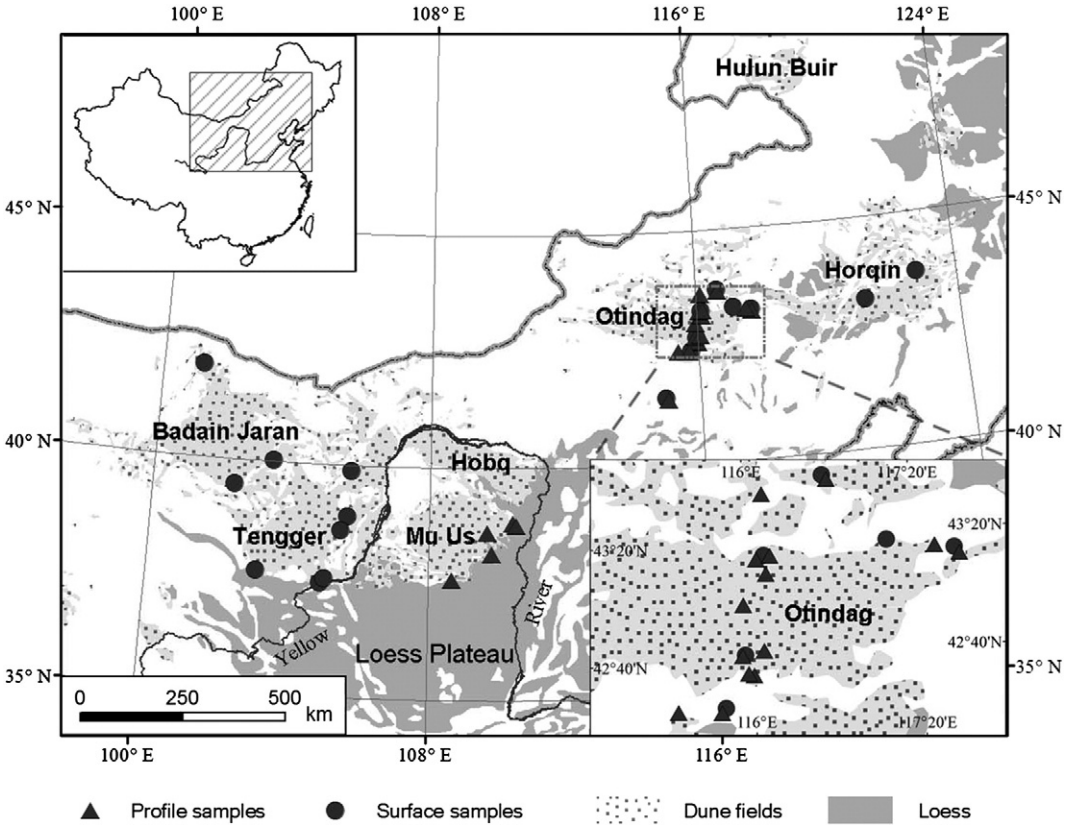

Figure 1. Sites of the surface and buried soil and sediment sampling in the Badain Jaran desert, Tengger desert, Otindag dune field, Mu Us dune field and Chinese Loess Plateau in northern China. The solid circle and triangle indicate the surface and section sampling sites, respectively.

https://doi.org/10.1016/j.yqres.2012.01.009 Published online by Cambridge University Press

Table 1
Carbon isotopic composition of surface samples from the Badain Jaran desert, the Tengger desert, the Otindag dune field, and the Horqin dune field. Both of the latitudes and longitudes of sampling sites are presented, with the laboratory numbers of the samples and the measurement errors (‰).

Series no.	Field record	Lab no.	GPS location	δ13C (VPDB)	Error (±)
Badain Jaran desert					
1	HYL interdune	10661	N41.99°, E101.18°, Alt.929 m	−24.91	0.013
2	HYL soil	10680	N41.99°, E101.18°, Alt.930 m	−23.96	0.021
3	HYL soil	10689	N41.99°, E101.18°, Alt.931 m	−23.11	0.011
4	BDJL S	10664	N39.47°, E102.37°, Alt.1431 m	−21.76	0.033
5	BDJL interdune	10693	N39.47°, E102.37°, Alt.1432 m	−22.86	0.019
6	XLBLG S	10683	N40.03°, E103.44°, Alt.1732 m	−23.98	0.023
7	BB S	10691	N37.64°, E103.11°, Alt.1732 m	−23.14	0.034
8	BB interdune	10714	N37.64°, E103.11°, Alt.1733 m	−23.49	0.005
Tegger desert					
9	X757 Road-6 km S	10658	N39.68°, E105.79°, Alt.1315 m	−22.31	0.007
10	X757 Road-134 km soil	10677	N39.88°, E105.71°, Alt.1024 m	−21.58	0.045
11	X757 Road 134 km S	10679	N39.88°, E105.71°, Alt.1025 m	−21.9	0.005
12	MJW S	10659	N37.45°, E104.93°, Alt.1424 m	−21.67	0.012
13	MJW interdune	10672-1	N37.45°, E104.93°, Alt.1425 m	−21.73	0.009
14	MJW-20.3 m soil	10667	N37.45°, E104.93°, Alt.1426 m	−20.38	0.022
15	DPL interdune	10660	N37.54°, E105.058°, Alt.1282 m	−23.48	0.001
16	DPL S	10690	N37.54°, E105.058°, Alt.1283 m	−23.46	0.038
17	HDM interdune	10670	N38.90°, E105.66°, Alt.1473 m	−23.3	0.001
18	HDM S	10686	N38.90°, E105.66°, Alt.1474 m	−22.54	0.002
19	YLH S	10672	N38.58°, E105.48°, Alt.1283 m	−24.18	0.005
20	YLH interdune	10685	N38.58°, E105.48°, Alt.1284 m	−20.53	0.028
21	YLH S	10692	N38.58°, E105.48°, Alt.1285 m	−22.09	0.009
Otindag dune field					
22	303 Road 1interdune	10684	N43.30°, E117.12°, Alt.1289 m	−24.16	0.001
23	303 Road 1100 km S	10668	N43.30°, E117.12°, Alt.1290 m	−23.79	0.003
24	303 Road 55 km interdune	10666	N43.69°, E116.64°, Alt.1216 m	−23.41	0.002
25	303 Road 55 km S	10674	N43.69°, E116.64°, Alt.1217 m	−24.05	0.003
26	303 Road 55 km lamellae	10676	N43.69°, E116.64°, Alt.1218 m	−22.70	0.011
27	JPE S	10673R	N43.23°, E117.66°, Alt.1018 m	−23.14	0.004
28	JPE interdune	10665	N43.23°, E117.66°, Alt.1019 m	−24.02	0.021
29	HBRG S	10662	N42.40°, E115.77°, Alt.1378 m	−23.42	0.020
30	HSDKN S	10663	N43.25°, E116.13°, Alt.1302 m	−24.35	0.014
31	HSDKN soil	10671	N43.25°, E116.13°, Alt.1303 m	−24.34	0.034
32	HSDKN interdune	10687	N43.25°, E116.13°, Alt.1304 m	−24.04	0.005
33	SGDL S	10675	N42.69°, E115.95°, Alt.1328 m	−25.22	0.004
34	LW S	10688	N41.40°, E114.97°, Alt.1386 m	−22.78	0.003
Horqin dune field					
35	BXT S	10678	N43.22°, E121.16°, Alt.287 m	−20.14	0.003
37	D06-QG	HOR6	N42.84°, E119.45°, Alt.620 m	−20.55	0.041
38	D04-HLE	HOR4	N43.20°, E119.42°, Alt.475 m	−21.60	0.043
39	D02-WFD	HOR2	N 43.24°, E 118.61°, Alt.651 m	−21.52	0.043
40	D19-CS	HOR19	N 42.84°,122.49°, Alt.247 m	−20.36	0.040
41	D18-SD	HOR18	N 42.82°, E 123.03°, Alt.149 m	−19.47	0.038
42	D14-HLT	HOR14	N 43.29°, E123.02°, Alt.169 m	−19.09	0.038
43	D11	HOR11	N 43.90°, E121.07°, Alt.254 m	−20.13	0.040
44	D10-BGB	HOR10	N43.05°, E 120.38°, Alt.352 m	−23.54	0.047
45	D20-KLQ	HOR20	N42.73°, E121.69°, Alt.380 m	−21.75	0.044

using the C_4 photosynthetic pathway include 27 species in 7 families and 22 genera, indicating that the C_4 species mainly occurred in a few families; however, the C_4 are common plants and play an important role in overall vegetation changes (Wang, 2004).

The Horqin dune field (Fig. 1) has an area of 50,600 km^2 with a MAT of 6.9°C and MAP of 390 mm, in which 70–80% of the rain falls in June, July, and August. Dominant species include *Agriophyllum squarrosum* (a C_4 grass), *Salsola collina* (a C_4 herbaceous plant), *Setaria viridis* (a C_4 grass), *Artemisia halodendron* and *Cleistogenes squarrosa* (a C_4 grass) (Yin and Li, 1997), with scattered trees of *Pinus sylvestris var. mongolica*, *Populus simonii Carr.* and *Ulmus pumila* in the Dune field. More descriptions of the nature of these three dune fields are in Mason et al. (2008).

To investigate the relationships between surface soil organic carbon isotopic signatures and the associated climate and vegetation, 45 new surface samples were collected from the Otintag and Horqin dune fields and the more arid Tengger and Badain Jaran deserts (Fig. 1, specific locations in Table 1). All samples were collected from 2 to 4 cm below the natural surface of eolian deposits within 2–4 cm; anthropogenically disturbed surfaces were avoided when collecting these surface samples. In addition, the surface samples were from well-drained, porous sandy sediment and soils, presumably resulting in limited activity of cyanobacteria and aquatic organisms. Thus, those organisms make a negligible contribution to the soil organic carbon isotopic values (Wang et al., 2003), as do crassulacean acid metabolism (CAM) plants (Wang, 2004).

The sections in the Mu Us, Otindag and Horqin dune fields that were sampled for organic carbon isotopic analysis were well-exposed, with distinct alternations of soils marked by relatively thick dark A horizons, and eolian sand or sandy loess units. After excavating a 30–40 cm trough to avoid surface contamination, vertical sections were sampled based on stratigraphic observations in the field. As a result, 103 bulk sediment samples are collected and measured for stable carbon isotopic composition and other proxy indexes such as magnetic susceptibility, grain size distribution and total organic matter content (Table 2 and Fig. 2).

https://doi.org/10.1016/j.yqres.2012.01.009 Published online by Cambridge University Press

Table 2
The carbon isotopic composition of buried samples from the Mu Us and Otindag dune fields, and the magnetic susceptibility, grain size distribution and the total organic matter content, in which the carbon isotopic data, the total organic matter content of all the samples from the Otindag dune fields, and the magnetic susceptibility and grain size of sites of MJZ, 308 Road 132 km, HBRG, HSDK(N), SGDL s B, New 207 Road 116 km, JPHW, are firstly reported in this study; the ages and other proxy indicators have been reported (Lu et al., 2005; Zhou et al., 2008; Mason et al., 2009).

Series no.	Field record	Lab no.	$\delta^{13}C$ (‰)	ST error	OSL age (ka)	MS(SI)	GS (μm)	TOC (%)
Mu Us dune field								
1	DBY-30	10594	−19.87	0.008	7.39 ± 0.48	58.67	132.2	2.36
2	DBY-60	10595	−21.09	0.021	N/A	28.50	170.6	1.47
3	DBY-90	10596	−21.89	0.006	12.7 ± 1.1	17.83	237.5	0.55
4	DBY-120	10597	−22.94	0.020	N/A	8.83	334.3	0.18
5	DBY-150	10598	−23.67	0.005	13.65 ± 1.50	24.17	142.9	0.42
6	DBY-180	10599	−22.50	0.008	N/A	16.00	193.6	0.26
7	DBY-220	10600	−23.28	0.004	37.71 ± 2.75	13.17	82.2	0.30
8	DBY-270	10601	−22.54	0.011	N/A	21.50	94.6	0.25
9	DBY-310	10602	−23.05	0.003	52.05 ± 4.03	21.67	128.3	0.26
10	DBY-380	10603	−23.80	0.010	N/A	16.00	133.7	0.34
11	SDG-40	10649	−23.34	0.015	7.56 ± 0.58	40.67	120.9	1.24
12	SDG-80	10650	−23.84	0.021	8.10 ± 0.57	70.83	91.1	1.59
13	SDG-160	10651	−24.01	0.006	8.38 ± 0.55	20.67	126.0	0.94
14	SDG-220	10652	−23.09	0.015	9.78 ± 0.63	20.00	154.3	0.19
15	SDG-280	10653	−23.68	0.020	11.0 ± 0.84	32.67	80.9	0.40
16	SDG-320	10654	−21.93	0.010	41.84 ± 2.59	34.00	39.9	1.13
17	CJG-40	10636	−21.07	0.023	7.29 ± 0.33	69.00	90.0	1.57
18	CJG-80	10637	−22.35	0.001	7.81 ± 0.50	49.33	109.0	1.57
19	CJG-130	10638	−23.76	0.006	8.55 ± 0.48	28.00	125.3	0.51
20	CJG-220	10639	−23.85	0.016	9.98 ± 0.61	13.50	177.3	0.20
21	YYC-1	10628	−24.77	0.022	0.29 ± 0.05	2.00	211.7	0.15
22	YYC-2	10629	−25.68	0.015	N/A	3.00	197.9	0.27
23	YYC-3	10630	−21.17	0.036	N/A	14.00	119.5	0.45
24	YYC-4	10631	−21.89	0.022	N/A	9.00	137.0	0.37
25	YYC-5	10632	−23.56	0.040	2.39 ± 0.14	4.00	205.1	0.26
26	YYC-6	10633	−24.16	0.023	N/A	3.00	163.1	0.18
27	JB-30	10634	−22.59	0.014	N/A	35.00	34.4	0.98
28	JB-510	10635	−23.43	0.008	7.56 ± 0.57	21.67	45.0	0.23
Otindag dune field								
29	LW–0.65 m	10517	−23.08	0.007	4.46 ± 0.22	24.80	121.4	0.59
30	LW–2 m	10540	−23.19	0.016	7.96 ± 0.42	30.15	166.0	0.65
31	308 Road 132 km–0.6 m	10539	−23.33	0.018	0.74 ± 0.04	23.00	167.2	0.95
32	308 Road 132 km–1.6 m	10538	−23.52	0.007	0.95 ± 0.05	23.50	131.8	0.50
33	SGDLs-A–2 m	10542R	−23.60	0.003	0.43 ± 0.03	12.90	258.0	0.82
34	SGDLs-A–2.65 m	10543	−24.61	0.026	0.66 ± 0.04	12.50	200.5	0.71
35	SGDLs-A–3.2 m	10544	−23.94	0.026	N/A	11.85	188.1	0.32
36	SGDLs-A–3.6 m	10545	−23.99	0.012	1.30 ± 0.07	9.60	237.0	0.73
37	SGDLs-A–4.0 m	10546	−24.62	0.014	N/A	20.15	180.5	0.44
38	SGDLs-B–2.2 m	10524	−23.18	0.024	2.76 ± 0.15	6.60	222.5	0.53
39	SGDLs-B–3.1 m	10514	−23.25	0.015	4.48 ± 0.24	20.40	183.9	1.14
40	SGDLs-B–6.3 m	10525	−23.50	0.009	17.73 ± 0.92	10.50	174.8	0.44
41	SGDL–0.5 m	10513R	−24.59	0.028	0.13 ± 0.01	6.65	218.9	0.81
42	SGDL–1.4 m	10526	−23.77	0.025	0.63 ± 0.04	5.70	340.9	0.73
43	SGDL–3.0 m	10527	−24.63	0.006	0.68 ± 0.04	9.90	250.2	0.88
44	SGDL–5.65 m	10528	−23.61	0.004	4.04 ± 0.22	11.75	195.2	1.22
45	SGDL–5.85 m	10529	−23.82	0.016	N/A	13.70	203.2	1.47
46	SGDL–6.40 m	10530	−24.48	0.033	N/A	2.05	328.5	0.31
47	SGDL–7.35 m	10531	−24.84	0.022	9.90 ± 0.55	1.40	271.6	0.44
48	JPHW–3 m	10535	−23.82	0.020	N/A	9.45	202.6	0.56
49	JPHW–8.5 m	10536	−24.64	0.020	N/A	2.40	223.7	0.33
50	JPHW–9.5 m	10537	−24.97	0.033	8.21 ± 0.24	21.25	215.3	0.73
51	New 207 Road 116 km–1.0 m	10520	−23.45	0.040	0.49 ± 0.03	9.10	245.7	0.69
52	New 207 Road 116 km–1.6 m	10521	−23.77	0.024	N/A	9.40	244.6	0.26
53	New 207 Road 116 km–6.0 m	10522	−22.81	0.074	0.63 ± 0.04	10.30	309.2	0.51
54	New 207 Road 116 km–8.0 m	10523	−23.57	0.033	0.63 ± 0.04	8.45	272.4	0.32
55	207 Road 87 km–14 m	10573	−23.21	0.041	5.24 ± 0.28	3.40	228.4	0.72
56	207 Road 87 km–15.3 m	10574	−24.13	0.021	6.64 ± 0.37	6.10	217.6	0.81
57	207 Road 87 km–8.5 m	10575	−24.21	0.007	2.34 ± 0.12	5.75	221.1	1.72
58	207 Road 87 km–9.5 m	10576	−24.15	0.030	4.97 ± 0.27	4.70	236.2	0.65
59	207 Road 87 km–20.3 m	10577	−25.01	0.024	8.88 ± 0.47	2.25	280.8	0.50
60	HSHN-01	10640	−24.92	0.004	0.14 ± 0.01	8.55	241.5	0.48
61	HSHN-02	10641	−23.98	0.019	2.70 ± 0.11	26.90	201.4	1.95
62	HSHN-03	10642	−23.13	0.001	5.02 ± 0.38	40.30	204.7	4.01
63	HSHN-04	10643	−23.39	0.016	7.73 ± 0.36	10.30	295.6 1.60	
64	303 Road 55 km–3.0 m	10551	−23.83	0.004	1.62 ± 0.09	7.35	335.1	0.73
65	303 Road 55 km–3.5 m	10552	−23.00	0.001	N/A	14.50	266.3	0.68
66	303 Road 55 km–4.5 m	10553	−23.53	0.014	8.68 ± 0.47	6.25	310.5	1.33
67	303 Road 55 km–6 m	10554	−23.91	0.025	N/A	5.55	338.3	0.24
68	303 Road 55 km–8 m	10555	−23.94	0.004	9.37 ± 0.50	5.55	364.4	0.51
69	JPE–1.0 m	10565	−22.97	0.008	2.03 ± 0.13	7.90	261.2	0.35

https://doi.org/10.1016/j.yqres.2012.01.009 Published online by Cambridge University Press

Table 2 (*continued*)

Series no.	Field record	Lab no.	$\delta^{13}C$ (‰)	ST error	OSL age (ka)	MS(SI)	GS (μm)	TOC (%)
70	JPE–2.3 m	10566	−23.33	0.020	2.73 ± 0.15	7.70	360.3	0.84
71	JPE–3.4 m	10567	−23.61	0.027	3.32 ± 0.20	4.90	343.4	1.11
72	JPE–4.5 m	10568	−22.78	0.014	1.58 ± 0.10	10.40	234.9	0.94
73	JPE–4.9 m	10569	−23.32	0.019	1.22 ± 0.08	3.95	354.2	1.03
74	MJZ–01	10644	−24.62	0.015	0.71 ± 0.03	4.10	229.4	2.14
75	MJZ–02	10645	−25.06	0.018	1.53 ± 0.12	12.35	172.2	3.29
76	MJZ–03	10646	−24.90	0.022	4.06 ± 0.09	3.95	134.5	2.94
77	MJZ–04	10647	−24.32	0.036	8.72 ± 0.16	2.10	253.7	1.56
78	MJZ–05	10648	−24.62	0.028	8.74 ± 0.35	3.60	150.1	1.55
79	207 Road 38 km–3 m	10623	−24.39	0.013	N/A	11.40	318.0	0.38
80	207 Road 38 km–8.7 m	10627	−22.42	0.025	N/A	12.85	223.2	0.24
81	HSDK(N)–1.25 m	10547	−23.13	0.021	The HSHN site	42.80	142.5	1.21
82	HSDK(N)–6.3 m	10548R	−24.45	0.003	The HSHN site	4.70	296.2	0.90
83	HBRG–0.4 m	10541	−23.65	0.012	N/A	44.25	36.8	1.48
84	HBRG–2.3 m	10516	−22.91	0.007	N/A	39.35	57.0	0.21
Horqin dune field								
86	SJZ–0.7 m	10604	−20.94	0.006	N/A	20.90	163.5	1.09
87	SJZ–1.4 m	10605	−20.90	0.025	N/A	19.70	113.6	0.87
88	SJZ–1.9 m	10606	−20.50	0.005	0.76 ± 0.05	19.65	125.7	0.88
89	SJZ–3.0 m	10607	−20.31	0.007	19.55 ± 1.50	24.55	104.2	1.67
90	SJZ–4.6 m	10608	−22.31	0.017	N/A	24.05	82.2	0.84
91	SJZ–6.6 m	10609	−21.97	0.017	N/A	36.80	51.4	0.47
92	SLL–1.2 m	10558	−22.19	0.038	N/A	3.25	294.2	0.76
93	SLL–3.8 m	10559	−23.42	0.011	N/A	4.05	261.8	0.79
94	SLL–5.6 m	10560	−21.98	0.034	N/A	3.80	289.4	1.05
95	SLL–6.8 m	10561	−21.91	0.050	N/A	3.85	252.2	0.79
96	SLL–7.4 m	10562	−21.95	0.019	N/A	3.45	233.5	0.81
97	SLL–12.3 m	10563	−22.21	0.023	N/A	2.35	246.3	0.79
98	SLL–15.8 m	10564	−25.00	0.012	10.80 ± 0.92	1.20	273.0	0.80
99	BXT–1.0 m	10614	−21.84	0.026	N/A	5.45	272.0	0.31
100	BXT–2.0 m	10615	−22.69	0.008	N/A	4.40	297.3	0.24
101	BXT–2.9 m	10616	−22.06	0.008	N/A	7.10	265.3	0.24
102	BXT–5.4 m	10617	−19.54	0.014	3.15 ± 0.24	28.25	176.4	1.11
103	BXT–6.8 m	10618	−22.49	0.036	10.31 ± 0.82	1.30	325.8	0.22

Age control for these stratigraphic sections is based on optically stimulated luminescence (OSL) ages, all previously published (Lu et al., 2005; Zhou et al., 2008, 2009; Mason et al., 2009). The OSL ages of eolian sediments primarily record the time of deposition, although ages from buried soils may be somewhat younger than the time of deposition because of light exposure through bioturbation (Mason et al., 2009; Lu et al., 2011).

3. Laboratory methods and data analysis

For stable carbon isotope analysis of organic matter in these sediments and soils, visible roots of modern plants were removed by hand, the analyzed samples were dried at 50°C for 24 h, ~3 g of ground soil (<75 μm) was treated with 2 mol L^{-1} HCl for 24 h at room temperature to remove carbonates. Then, the sample was washed to pH > 7 with distilled water and dried at 50°C. Subsamples of about 0.1 g were used for carbon isotopic analysis. The samples were combusted for 4 h at 850°C in an evacuated sealed quartz tube in the presence of silver foil and cupric oxide. The purified carbon oxide was then analyzed for carbon isotopes using a MAT-251 gas mass spectrometer with dual inlet system. Isotopic ratios in samples are expressed as per mil deviations relative to a VPDB standard, with a precision better than 0.4‰.

The magnetic susceptibility (MS), grain size distribution (GS) and total organic matter content (TOC) have been previously reported (Lu et al., 2005; Zhou et al., 2008) except for data from the following sites: MJZ, 308 Road 132 km, HBRG, HSDK(N), SGDL s B, New 207 Road 116 km, JPHW (Table 2). Methods for the new measurements were identical to those described previously (Lu et al., 2005; Zhou et al., 2008). Typical examples of the stratigraphy of the sections studied, and the sampling strategy used for MS, GS and TOC measurements are presented in Figure 3.

To analyze the relationship between surface sample δ^{13} C and climate, MAT and MAP values were obtained for the weather station nearest each sampling site from the Data Center, China Meteorological Bureau. We then tested linear models in which $\delta^{13}C$ is a function of MAP and/or MAT. We used t-tests to assess whether mean $\delta^{13}C$ values from surface samples differed between Dune fields, and also whether mean $\delta^{13}C$ values for paleosol samples differed from means for unweathered eolian sand within individual dune fields. All statistical analyses were carried out in R (Ihaka and Gentleman, 1996).

The relative abundance of C_4 plants as a percentage of total vegetation biomass can be estimated using equations such as the one proposed by Vidic and Montañez (2004) for the Loess Plateau: % $C_4 = 100 * (27 + \delta^{13}C)/14$; where the average carbon isotope value of C_3 plants is −27‰ and that of C_4 plants is −14‰. Although equations of this type are widely used (e.g., Nordt et al., 2008), the uncertainty of the resulting % C_4 values is large and difficult to estimate. Both the mean and variance of $\delta^{13}C$ values for plants using both photosynthetic pathways vary spatially and temporally in response to climate and other factors (Pyankov et al., 2000; Wittmer et al., 2008; Auerswald et al., 2009; Diefendorf et al., 2010). These equations also do not account for changing $\delta^{13}C$ when plant material is decomposed in soils and sediments, an effect that will vary with depth below the soil surface and other factors (Melillo et al., 1989; Wedin et al., 1995; Wiesenberg et al., 2004; Liu and Huang, 2008).

4. Results

Of the four dune fields and deserts where new surface soil samples were collected, the mean value of $\delta^{13}C$ was highest for the relatively warm and subhumid Horqin dune field (mean ± standard deviation of −20.8 ± 1.3‰). The lowest mean surface soil $\delta^{13}C$ was −23.8 ± 0.7‰ in the cold semiarid Otindag dune field, while surface sample

https://doi.org/10.1016/j.yqres.2012.01.009 Published online by Cambridge University Press

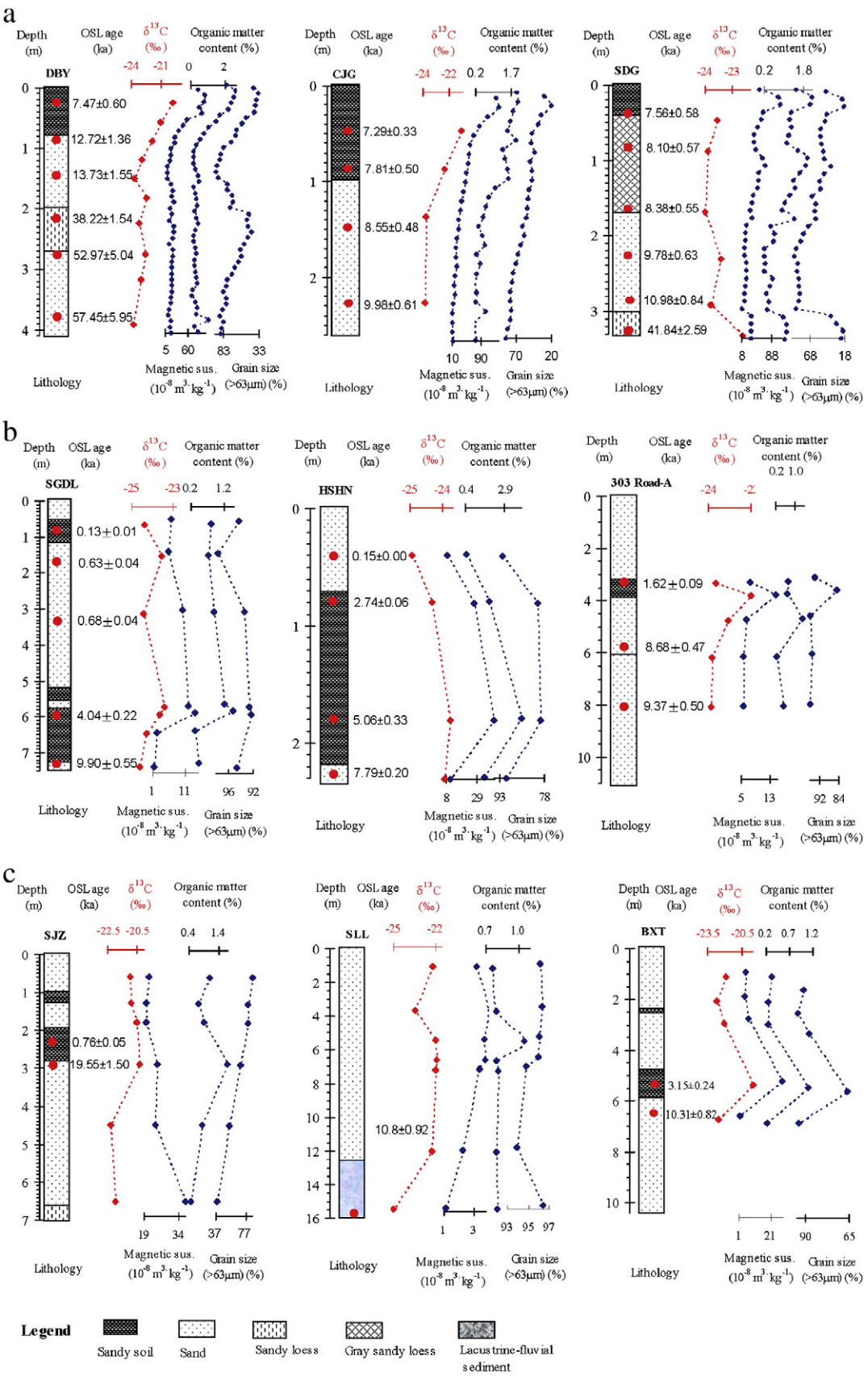

Figure 2. Carbon isotopic composition variations in the typical sand dune sections in the Mu Us dune field (DBY, CJG, SDG), the Otindag dune field (SGDL, HSHN, 303 Road-A) and the Horqin dune fields (SJZ, SLL, BXT), showing general co-variations of the carbon isotopic compositions and other proxy indices of pedogenesis and climate. The data of all the 20 sections are shown in Table 2.

https://doi.org/10.1016/j.yqres.2012.01.009 Published online by Cambridge University Press

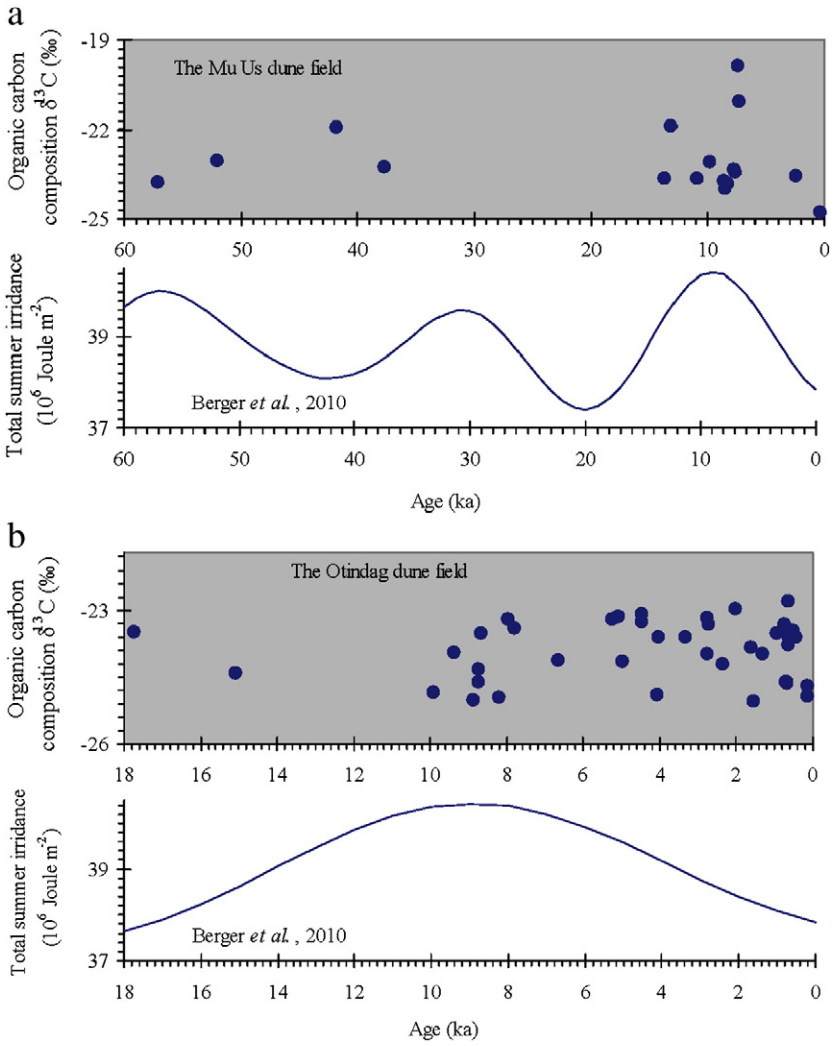

Figure 3. $\delta^{13}C$ values, plotted against OSL at the same depth of in eolian stratigraphic sections of the Mu Us and Otindag dune fields. Total summer insolation (Berger et al., 2010) is shown for comparison.

means from the Badain Jaran and Tengger deserts are intermediate (-23.4 ± 0.9‰ and -22.2 ± 1.1‰, respectively. The raw $\delta^{13}C$ values approximate normal distributions (as a whole and by dune field) based on Q–Q plots, so they were not transformed before statistical analysis. Based on two-tailed t-tests, mean values for all four dune fields and deserts were significantly different ($p<0.05$) from each other, except for the Otindag dune field and Badain Jaran desert. Using the Vidic and Montañez (2004) equation, the mean $\delta^{13}C$ values yield relative C_4 estimates from 23% (Otindag) to 44% (Horqin).

For all surface samples collected in this study ($n=45$), $\delta^{13}C$ is very weakly related to MAT alone ($R^2=0.139$, $p<0.05$), and there is no significant relationship with MAP alone. However, using the best-fit model for $\delta^{13}C$ as a function of both MAT and MAP, the multiple R^2 is 0.527 (adjusted $R^2=0.504$; see Table 3 for summary):

$$\delta^{13}C = -28.9 + 0.541\mathrm{MAT} + 0.012\mathrm{MAP}.$$

This model is consistent with the variation of mean surface sample $\delta^{13}C$ among the various dune fields and deserts, showing that $\delta^{13}C$ increases with both MAT and MAP. We also tried pooling our new data with $\delta^{13}C$ values from surface samples in the Loess Plateau reported by Liu et al. (2005a), but for the combined data set there are no significant relationships with MAT and/or MAP.

In stratigraphic sections of the Mu Us, Otindag, and Horqin dune fields, paleosols identified in the field consistently have higher organic carbon content and magnetic susceptibility, and lower coarse particle content, than eolian sands or loess that lack pedogenic alteration (examples in Fig. 2). In the Mu Us and Horqin dune fields, $\delta^{13}C$ values of organic carbon increase in paleosols as well. In both of these dune fields, t-tests indicate that the mean $\delta^{13}C$ in paleosols is significantly different ($p<0.05$) from the mean value for unweathered eolian sand (-21.2 ± 1.2‰ for paleosols vs. -22.8 ± 1.1‰ for sand in Mu Us; -20.3 ± 0.7‰ for paleosols vs. -22.0 ± 0.7‰ for sand in Horqin). These differences correspond to about 11–12% increase in C_4 plants at time of paleosol formation. In contrast, the mean $\delta^{13}C$ is identical for paleosols and unweathered sand in the Otindag dune field (-23.9 ± 0.6‰ and -23.9 ± 0.8‰, respectively), as illustrated by sections shown in Figure 2b.

Table 3
Summary of linear model relating organic carbon $\delta^{13}C$ of surface samples to mean annual temperature and precipitation.

Coefficients	Estimate	Std. error	t value	*p*
(Intercept)	−28.9	0.95	−30.372	<0.001
MAT	0.54	0.08	6.428	<0.001
MAP	0.01	0.002	5.803	<0.001

Residual standard error: 1.075 on 41 degrees of freedom.
Multiple R^2: 0.527, Adjusted R^2: 0.504.
F-statistic: 22.88 on 2 and 41 DF, p-value: <0.001.

https://doi.org/10.1016/j.yqres.2012.01.009 Published online by Cambridge University Press

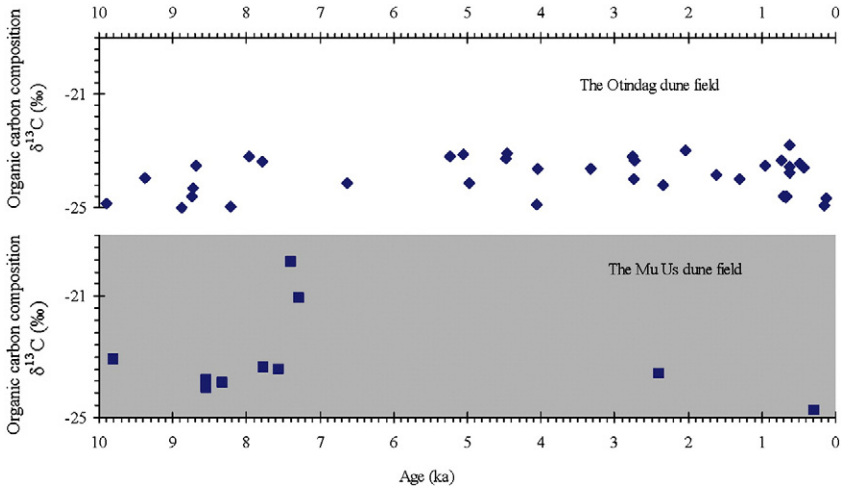

Figure 4. Same as Figure 3, but for the past 10,000 yr only.

In the Mu Us and Otindag dune fields, many of the samples used for isotopic analysis were collected from approximately the same depth as OSL dating samples, and for those samples, $\delta^{13}C$ is plotted against OSL age in Figures 3 and 4. In the Mu Us dune field, the $\delta^{13}C$ values corresponding to ages of 7–8 ka, all from paleosols, are higher than most other samples across the period from 60 to 0 ka. In the Otindag dune field, most samples with especially low $\delta^{13}C$ (<−24.5‰) correspond to OSL ages of 10–8 ka and 2–0 ka.

5. Carbon isotopic composition of surface samples, climate, and vegetation

The relationship between the carbon isotopic composition of surface sample organic matter, temperature, and precipitation is weak; however, it is consistent with the expected increase of C_4 vegetation in response to increasing temperature and precipitation in this setting, as reviewed above. In the Otindag dune field, low temperature limits the abundance of C_4 plants, and the $\delta^{13}C$ of surface samples reflects predominance of organic carbon derived from C_3 plants. In the warmer Horqin dune field, C_4 plants (mainly grasses) are much more abundant, also reflected in surface sample $\delta^{13}C$. In the arid Tengger and Badain Jaran deserts, field observations indicate that grasses are a less important component of the vegetation, probably reducing the overall abundance of C_4 plants despite the warm temperatures. More data on plant community composition and photosynthetic pathways of common species near our Tengger and Badain Jaran desert sampling sites would be needed to test that interpretation.

The large proportion (~50%) of total variance in surface sample $\delta^{13}C$ that cannot be explained by MAT and MAP only may be partly related to vegetation disturbance and succession resulting from patchy eolian activity and succession following restabilization of active sand, common in all the areas that were sampled. Recent biological investigations along the southeastern margin of the Tengger desert and the Horqin dune field found an increase in C_4 species abundance associated with increasing dune stability within areas of fairly uniform climate (Zhang et al., 2004; Zhao et al., 2009).

The inferred relationship between climate, C_4 plant abundance, and $\delta^{13}C$ is specific to the deserts and semiarid dune fields that we studied. As noted above, it does not appear to apply to the samples of Liu et al. (2005a) from across the Loess Plateau. The Loess Plateau has a long history of intensive human land use, so surface samples may be influenced by past input of carbon from C_3 trees and crops such as wheat, even if the sampling sites are now under natural vegetation. Data from another study suggest a more general effect, however, in which the positive relationship between MAP and $\delta^{13}C$ in surface soils is reversed above a certain level of precipitation. Feng et al. (2008) report organic carbon isotopic analyses along a transect from Mongolia southward across the Loess Plateau, spanning a much larger range of climate and vegetation. For their transect as a whole, they found negative correlations between surface-soil organic $\delta^{13}C$ values and both MAP ($R^2=0.453$; $n=196$; $p<0.05$) and growing-season (April–September) precipitation ($R^2=0.497$; $n=196$; $p<0.05$). These relationships are strongly influenced by the low $\delta^{13}C$ values obtained at the northern and southern ends of their transect, however, where forest (virtually all C_3 plants) is present today or was present in the past. In fact, a detailed look at the data of Feng et al. (2008) shows that the highest $\delta^{13}C$, indicating greatest C_4 abundance, occurs in semi-arid to subhumid areas with desert-steppe or steppe vegetation, not in the most arid portion of the transect. This pattern is similar to that observed in our surface samples, with higher $\delta^{13}C$ in the subhumid Horqin dune field than in the arid Badain Jaran and Tengger desert.

6. Late Quaternary variations of carbon isotopic composition in the Mu Us, Otindag, and Horqin dune fields

We interpret variation of carbon isotopic data from stratigraphic profiles in the context of previous research on the late Quaternary record of environmental change in these three dune fields. Paleosols are interpreted as representing dune stabilization at times when the climate was relatively humid; eolian sand units are interpreted as representing dry climatic conditions, and when temperatures were probably lower (Dong, 2002; Lu et al., 2005; Zhou et al., 2008; Mason et al., 2009; He et al., 2010). Based on OSL dating of stratigraphic sections containing eolian sediments and paleosols at many sites, widespread dune activity occurred across all three dune fields at 11.5 to 8 ka (possibly beginning earlier), followed by widespread stabilization and soil formation in the middle Holocene. The major soils in sections shown in Figure 2 formed at that time; note that soils shown at the top of the DBY, and CJG, and SDG sections (Fig. 2a) are correlated with a widespread soil buried by late Holocene sands in nearby sections. The OSL ages from those soils, between 7 and 8 ka, may represent the last increment of sand deposition as stabilization began, and soil formation probably continued into the late Holocene (see Mason et al., 2009 and Lu et al., 2011 for more thorough discussion). Extensive dune reactivation occurred in the late Holocene, especially since 1 ka (Lu et al., 2005; Zhou et al., 2008; Mason et al., 2009; Lu et al., 2011).

The abundant organic carbon used for isotopic analysis in the paleosols clearly accumulated after sand deposition and represents organic matter input from vegetation growing on those soils. As

https://doi.org/10.1016/j.yqres.2012.01.009 Published online by Cambridge University Press

noted above, interpretation of OSL ages from the paleosols is complex, but their organic carbon should represent vegetation during the general period of soil formation and dune field stability as inferred from multiple sites and OSL ages. We assume that organic carbon in unweathered eolian sands was also mainly added after deposition, because organic matter and other fines are probably quickly removed from saltating sand grains by abrasion and winnowing. Some vegetation was probably always present on parts of the dunes even at times of extensive activity, because Holocene dune activity in all three fields often involved parabolic dunes or sand sheets associated with partial vegetation cover (Lu et al., 2011). We use the OSL ages (recording deposition) as a rough indicator of the organic carbon age in the rapidly accumulated eolian sands because the lag between the two is probably short, an assumption that may be testable by radiocarbon dating in future work.

Climatic change is the most obvious explanation for the small but significant difference in carbon isotopic composition between paleosols and unweathered eolian sand in the Mu Us and Horqin dune fields. In this explanation, the higher values of $\delta^{13}C$ in the paleosols records increased abundance of C_4 plants when the climate favored dune stabilization and soil formation. Greater effective moisture clearly played a role in stabilizing the dunes, and both surface sample $\delta^{13}C$ and modern C_4 plant abundance in the Mu Us dune field (Yin and Li, 1997) increase with precipitation. The relationship between surface sample $\delta^{13}C$ and MAT, and the general response of C_4 plants to increasing temperature, raise the possibility that high temperature also favored C_4 expansion during the early to middle Holocene period of dune stabilization and soil formation.

The lack of a difference in $\delta^{13}C$ between paleosols and eolian sand in the Otindag dune field may be explained by a temperature limitation on vegetation response to climate change in that cold setting. That is, both precipitation and temperature might have increased significantly in the Otindag region at times of soil formation, but no response is recorded by stable carbon isotopes because the temperature was still cold enough to limit C_4 expansion. On the other hand, greater range and lower minimum values of $\delta^{13}C$ at 10–8 and 1–0 ka in the Otindag dune field (Figs. 3, 4) may record some response by vegetation to drier and possibly colder conditions during those times of dune activity.

In addition to direct effects of climate, C_4 plants might have been favored during times of dune stability by the lack of disturbance related to blowing sand and wind erosion, as suggested by modern observations discussed above. In the U.S. Great Plains, a shift toward lower abundance of C_4 grasses during periods of greater eolian activity in the early Holocene was similarly interpreted as an effect of increased disturbance (Feggestad et al., 2004).

Given the relatively small difference in $\delta^{13}C$ (1–3‰) between paleosols and eolian sands in the Mu Us and Horqin regions, we also must consider the effect of C isotope fractionation during decomposition, as discussed in the Introduction. This effect is typically expected to produce trends of *increasing* $\delta^{13}C$ with depth in a soil profile because organic matter deeper in the profile is more humified (Natelhoffer and Fry, 1988; Wynn et al., 2005, 2006; Boström et al., 2007); however, the opposite trend is observed in thick paleosol profiles in the Mu Us dune field (Fig. 2a, profiles DBY and CJG). Furthermore, there is no depth trend of $\delta^{13}C$ at all in paleosols of the Otindag dune field. Both of these observations suggest that decomposition effects do not make a substantial contribution to the shifts of $\delta^{13}C$ in the Mu Us and Horqin dune field sections, and support the interpretation of these shifts as primarily related to vegetation change.

The last glacial maximum (LGM) would be a good test of vegetation response to climate, but it is poorly represented by our data from the dune fields. Previously reported stable carbon isotope values in organic matter from a loess–paleosol sequence along the margin of the Mu Us dune fields at Huanxian (Liu et al., 2005b) provide information on that time period, however. Our new closely spaced OSL dating has been carried out at this section (Lu et al., 2006; Stevens et al., 2006), providing numerical age control for the $\delta^{13}C$ values (Fig. 5). This time series shows that the abundance of C_4 plants was low under the cold dry conditions in the LGM when the monsoon circulation was weak and higher during the warmer and more humid early Holocene (8–9 ka) when the monsoon was stronger.

7. Relationship of vegetation change to change in CO_2, monsoon strength, and insolation

Over the late Quaternary, changes in relative abundance of C_3 and C_4 plants may occur in response to climate or CO_2 changes, or both.

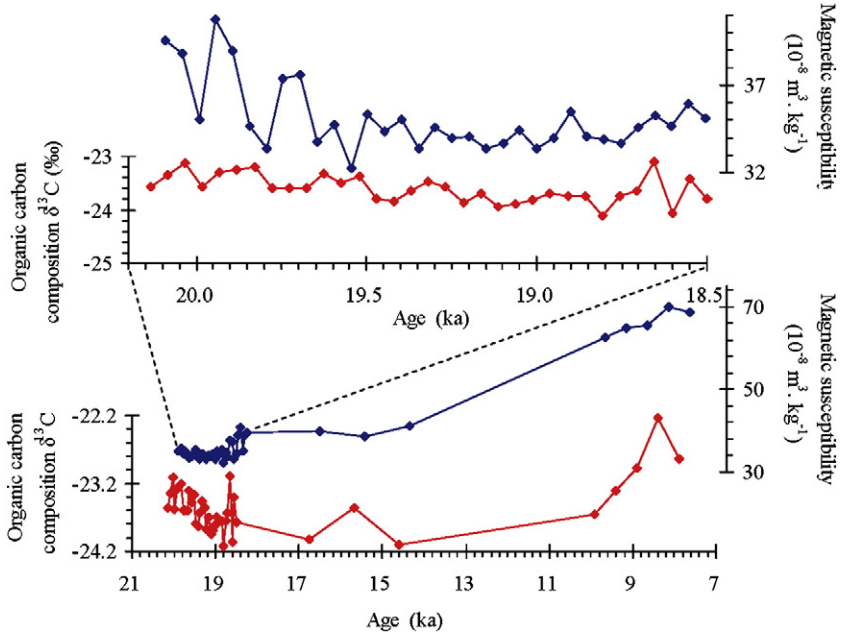

Figure 5. Variations of $\delta^{13}C$ values in the Huanxian loess–paleosol sequence near the margin of the Mu Us dune fields during the past 20 ka, with age control provided by closely spaced OSL dating (Liu et al., 2005a, 2005b; Lu et al., 2006; Stevens et al., 2006).

https://doi.org/10.1016/j.yqres.2012.01.009 Published online by Cambridge University Press

The temperature and precipitation are two major limits on the vegetation changes discussed above. During the Holocene, changes in CO_2 have been minor (Stauffer et al., 1998), and neither our new data nor the data from the Huanxian loess profile (Fig. 5) provide evidence for expansion of C_4 plants when CO_2 levels were lower in the late Pleistocene; therefore CO_2 forcing is not further discussed here.

Above, we proposed that isotopic data in at least two dune fields indicates greater C_4 plant abundance when the dune fields were stable than when they were active, suggesting a vegetation response primarily to changes in effective moisture. The timing of moisture variation reconstructed from eolian records in the dune fields and desert margin region of northern China is not in phase with reconstructions of summer monsoon strength in southern China. That is, while monsoon precipitation is believed to have peaked near the beginning of the Holocene in the south, the desert margin was dry then and became wet only after about 8 ka (Lu et al., 2005; Zhou et al., 2008; Mason et al., 2009). At the same time, the surface samples indicate a response of $\delta^{13}C$ to temperature, probably due to the greater competitive advantage of C_4 plants at higher temperatures. Many researchers have emphasized temperature as the predominant influence on C_4 plant distributions (Zhang et al., 2003). Summer insolation is often seen as the driver of change in the monsoon system, but also should have more direct effects on summer temperature. Therefore, we compared our isotopic data with the newly obtained total summer insolation (Berger et al., 2010) to evaluate whether those data provide any evidence of response to insolation-driven temperature change as well as moisture (Figs. 3, 4).

In the Mu Us dune field, several high $\delta^{13}C$ values suggest relatively high C_4 plant abundance in the early to mid-Holocene when insolation was high (Figs. 3, 4). Some of these measurements are from soils, and there is substantial uncertainty in estimating the time represented by organic carbon in the soils. Still, it is clear that dune field stabilization around 8 ka occurred while insolation was still high, and expansion of C_4 plants during formation of middle Holocene paleosols could have been driven by a combination of increased moisture and generally high temperature. The isotopic record from the Huanxian loess section just south of the Mu Us dune field also shows especially high $\delta^{13}C$, indicating high C_4 abundance, in the early Holocene (Fig. 5). Comparison of isotopic data from the Otindag dune field with insolation does not provide evidence for an insolation-driven temperature effect, however. The lowest $\delta^{13}C$ values occur at times of highest and lowest insolation during the Holocene (10–8 ka and 1–0 ka, respectively).

Further progress in identifying climatic controls on late Quaternary variation of C_4 and C_3 plant abundance could be made by radiocarbon dating of organic matter used for isotopic analysis, rather than relying entirely on the OSL chronology. Detailed studies of dated organic matter within the thick early-middle paleosols of the dunes in Mu Us dune field could be especially useful.

8. Conclusions

Carbon isotope analyses of organic matter in surface samples shows substantial variation in the relative abundance of C_4 and C_3 plants across the dune fields and deserts of northern China, about half of which can be explained as a response to mean annual temperature and precipitation. In stratigraphic sections of the Mu Us and Horqin dune fields, we found that increased $\delta^{13}C$, which we attribute to C_4 plant expansion, was associated with periods of dune stabilization and soil formation. A lower proportion of C_4 plants are often indicated by $\delta^{13}C$ values from eolian sand units, deposited during times of dune activity. Frequent disturbance during times of eolian activity may also have led to a lower proportion of C_4 plants. Stability and activity of these dune fields are primarily related to effective moisture, so changing moisture is clearly one factor that can explain changing C_4 plant abundance in the late Quaternary. However, the paleosols of the Mu Us and Horqin dune fields that have relatively high $\delta^{13}C$ also often started to develop in the early Holocene when insolation was high, and resulting high temperatures would have favored C_4 expansion at that time as well. Isotopic data from the Otindag dune field do not indicate increased C_4 plant abundance at times of dune stabilization. The Otindag region is much colder than the other dune fields, so C_4 expansion there was probably limited by low temperature throughout the late Quaternary. This interpretation also implies a strong effect of temperature as well as moisture on C_4 plant distribution in the dune fields and deserts of northern China. While conclusions of this study are tentative, they do indicate a high potential for better understanding of climate and vegetation change in this region through investigation of stable carbon isotopes in organic matter.

Acknowledgments

We thank Professor Jay Quade, Dr. Yurena Yanes and an anonymous reviewer who help to improve this paper. We thank Shuangwen Yi, Yingyong Chen, Cunfa Zhao, Xiaodong Miao, James Swinehart, Xianyan Wang, Lingjuan Wen, Xuefeng Sun, Xueqing Du, Yunning Cao and Chuanbin Yang for their help in field and laboratory work; we are grateful to Fangying Zhu for her help on the climatic data analysis. This research is funded by the Global Changes Program of Ministry of Science and Technology of China (2010CB950203), the National Natural Science Foundation of China (40930103; 41021002), the US National Science Foundation (ATM-0502489, ATM-0502511) and the CAS Strategic Priority Research Program Grant No. XDA05120700.

References

An, Z.S., Huang, Y.S., Liu, W.G., Guo, Z.T., Clemens, S.C., Li, L., Prell, W.L., Ning, Y.F., Cai, Y.J., Zhou, W.J., Zhang, Q.L., Cao, Y.N., Qiang, X.K., Chang, H., Wu, Z.K., 2005. Multiple expansions of C4 plant biomass in East Asia since 7 Ma coupled with strengthened monsoon circulation. Geology 33, 705–708.

Auerswald, K., Wittmer, M., Tannel, T.M., Bai, Y.F., Schaufele, R., Schnyder, H., 2009. Large regional-scale variation in C3/C4 distribution pattern of Inner Mongolia steppe is revealed by grazer wool carbon isotope composition. Biogeosciences Discussions 6, 545–574.

Berger, A., Loutre, M.F., Yin, Q.Z., 2010. Total irradiation during any time interval of the year using elliptic integrals. Quaternary Science Reviews 29, 1968–1982.

Boström, B., Comstedt, D., Ekblad, A., 2007. Isotope fractionation and ^{13}C enrichment in soil profiles during the decomposition of soil organic matter. Oecologia 153, 89–98.

Cerling, T.E., 1984. The stable isotopic composition of modern soil carbonate and its relationship to climate. Earth and Planetary Science Letters 71, 229–240.

Cerling, T.E., Quade, J., Wang, Y., Bowman, J.R., 1989. Carbon isotopes in soils and paleosols as ecology and paleoecology indicators. Nature 341, 138–139.

Connin, S.L., 2001. Isotopic discrimination during long-term decomposition in an arid land ecosystem. Soil Biology & Biogeochemistry 33 (1), 41–51.

Diefendorf, A.F., Mueller, K.E., Wing, S.L., Koch, P.L., Freeman, K.H., 2010. Global patterns in leaf ^{13}C discrimination and implications for studies of past and future climate. Proceedings of the National Academy of Sciences 107, 5738–5743.

Dong, G.R., 2002. Climate and Environment Changes in Deserts of China. China Ocean Press, Beijing, pp. 212–232.

Ehleringer, J.R., Cerling, T.E., 2002. C_3 and C_4 photosynthesis. In: Mooney, Harold A., Canadell, Josep G. (Eds.), The Earth System: Biological and Ecological Dimensions of Global Environmental Change. : Encyclopedia of Global Environmental Change, vol. 2. John Wiley & Sons, Ltd, Chichester. ISBN: 0-471-97796-9, pp. 186–190. Editor-in-Chief Ted Munn.

Farquhar, G.D., Ehleringer, J.R., Hubick, K.T., 1989. Carbon isotope discrimination and photosynthesis. Annual Review of Plant Physiology and Plant Molecular Biology 40, 503–537.

Feggestad, A.J., Jacobs, P.M., Miao, X.D., Mason, J.A., 2004. Stable carbon isotope record of Holocene environmental change in the Central Great Plains. Physical Geography 25, 170–190.

Feng, Z.D., Wang, L.X., Ji, Y.H., Guo, L.L., Lee, X.Q., Dworkin, S.I., 2008. Climatic dependency of soil organic carbon isotopic composition along the S–N Transect from 34°N to 52°N in central-east Asia. Palaeogeography, Palaeoclimatology, Palaeoecology 257, 335–343.

Fredlund, G.G., Tieszen, L.L., 1997. Phytolith and carbon isotope evidence for late Quaternary vegetation and climate change in the southern Black Hills, South Dakota. Quaternary Research 47, 206–217.

Gu, Z.Y., Liu, Q., Xu, B., Han, J.M., Yang, S.L., Ding, Z.L., Liu, T.S., 2003. Climate as the dominant control on C_3 and C_4 plant abundance in the Loess Plateau: organic carbon

https://doi.org/10.1016/j.yqres.2012.01.009 Published online by Cambridge University Press

isotope evidence from the last glacial–interglacial loess–soil sequences. Chinese Science Bulletin 48 (12), 1271–1276.
Hattersley, P.W., 1983. The distribution of C3 and C4 grasses in Australia in relation to climate. Oecologia 57, 113–128.
He, Z., Zhou, J., Lai, Z.P., Yang, L.H., Liang, J.M., Long, H., Ou, X.J., 2010. Quartz OSL dating of sand dunes of Late Pleistocene in the Mu Us Desert in northern China. Quaternary Geochronology 5, 102–106.
Huang, F., Kealhofer, L., Xiong, S.F., Huang, F.B., 2005. Holocene grassland vegetation, climate and human impact in central eastern Inner Mongolia. Science in China: Earth Sciences 48 (7), 1025–1039.
Ihaka, R., Gentleman, R., 1996. R: a language for data analysis and graphics. Journal of Computational and Graphical Statistics 5, 299–314.
Johnson, W.C., Willey, K.L., Mason, J.A., May, D.W., 2007. Stratigraphy and environmental reconstruction at the middle Wisconsinan Gilman Canyon Formation type locality, Buzzard's Roost, southwestern Nebraska, USA. Quaternary Research 67, 474–486.
Li, C.Y., Xu, Z.L., Kong, Z.C., 2003. A preliminary investigation on the Holocene vegetation changes from pollen analysis in the Gaoximge section, Hunshandak sandy land. Acta Phytoecologica Sinica 27, 797–803.
Li, Z.X., Liao, Y.C., Bai, G.S., 2005. Characteristic and construction of vegetation in Maowusu Sandy Land. Bulletin of Soil and Water Conservation 25, 66–70.
Liu, W.G., Huang, Y.S., 2008. Reconstructing in-situ vegetation changes using carbon isotopic composition of biopolymeric residues in the central Chinese Loess Plateau. Chemical Geology 249, 348–356.
Liu, S.L., Wang, T., 2005. Characteristic of climatic change in the Otindag sandy land region. Journal of Desert Research 25, 557–562.
Liu, W.G., Ning, Y.F., An, Z.S., Wu, Z.H., Lu, H.Y., Cao, Y.N., 2005a. Carbon isotopic composition of modern soil and paleosol as a response to vegetation change on the China Loess Plateau. Science in China: Earth Sciences 48 (1), 93–99.
Liu, W.G., Huang, Y.S., An, Z.S., Clemens, S.C., Li, L., Prell, W.L., Ning, Y.F., 2005b. Summer monsoon intensity controls C_4/C_3 plant abundance during the last 35 ka in the Chinese Loess Plateau: carbon isotope evidence from bulk organic matter and individual leaf waxes. Palaeogeography, Palaeoclimatology, Palaeoecology 220, 243–254.
Liu, W.G., Huang, Y.S., 2008. Reconstructing in-situ vegetation dynamics using carbon isotopic composition of biopolymeric residues in the central Chinese Loess Plateau. Chemical Geology 249, 348–356.
Lu, H.Y., Miao, X.D., Zhou, Y.L., Mason, J., Swinehart, J., Zhang, J.F., Zhou, L.P., Yi, S.W., 2005. Late Quaternary aeolian activity in the Mu Us and Otindag dune fields (North China) and lagged response to insolation forcing. Geophysical Research Letters 32 (21), L21716. doi:10.1029/2005GL024560.
Lu, H.Y., Stevens, T., Yi, S.W., Sun, X.F., 2006. An erosional hiatus in Chinese loess sequences revealed by closely spaced optical dating. Chinese Science Bulletin 51, 2253–2259.
Lu, H.Y., Zhao, C.F., Mason, J., Yi, S.W., Zhao, H., Zhou, Y.L., Ji, J.F., Swinehart, J., Wang, C.M., 2011. Holocene climatic changes revealed by aeolian deposits from the Qinghai Lake area (northeastern Qinghai-Tibetan Plateau) and possible forcing mechanisms. The Holocene 21 (2), 297–304.
Lu, H.Y., Mason, J.A., Stevens, T., Zhou, Y.L., Yi, S.W., Miao, X.D., 2011. Response of surface processes to climatic change in the dune fields and Loess Plateau of North China during the late Quaternary. Earth Surface Processes and Landforms 36, 1590–1603.
Lv, D.R., Chen, Z.Z., Chen, J.Y., Wang, G.C., Ji, J.J., Chen, H., Liu, Z.L., Zhang, R.H., Qiao, J.S., Chen, Y.J., 2002. Composite study on Inner Mongolia semi-arid grassland soil-vegetation–atmosphere inter action (IMGRASS). Earth Science Frontiers 9 (2), 295–306.
Maher, B.A., Prospero, J.M., Mackie, D., Gaiero, D., Hesse, P.P., Balkanski, Y., 2010. Global connections between aeolian dust, climate and ocean biogeochemistry at the present day and at the last glacial maximum. Earth-Science Reviews 99 (1–2), 61–97.
Martin, J.H., Fitzwater, S.E., 1988. Iron deficiency limits phytoplankton growth in the north-east Pacific subarctic. Nature 331, 341–343. doi:10.1038/331341a0.
Mason, J.A., Swinehart, J.B., Lu, H.Y., Miao, X.D., Cha, P., Zhou, Y.L., 2008. Limited change in dune mobility in response to a large decrease in wind power in semi-arid northern China since the 1970s. Geomorphology 102, 351–363.
Mason, J.A., Lu, H.Y., Zhou, Y.L., Miao, X.D., Swinehart, J.B., Liu, Z.Y., Goble, R.J., Yi, S.W., 2009. Dune mobility and aridity at the desert margin of northern China at a time of peak monsoon strength. Geology 37, 947–950.
Melillo, J.M., Aber, J.D., Linkins, A.E., Ricca, A., Fry, B., Nadelhoffer, K.J., 1989. Carbon and nitrogen changes along the decay continuum: plant litter to soil organic matter. Plant and Soil 115, 189–198.
Natelhoffer, K.J., Fry, B., 1988. Controls on natural nitrogen-15 and carbon-13 in forest soils. Soil Science Society of America Journal 52, 1633–1640.
Nordt, L., Von Fischer, J., Tieszen, L., Tubbs, J., 2008. Coherent changes in relative C_4 plant productivity and climate during the late Quaternary in the North American Great Plains. Quaternary Science Reviews 27, 1600–1611.
Ode, D.J., Tieszen, L.L., Lerman, J.C., 1980. The seasonal contribution of C_3 and C_4 plant species to primary production in a mixed prairie. Ecology 61, 1304–1311.
O'Leary, M.H., 1988. Carbon isotopes in photosynthesis. Bioscience 38, 328–336.
Pyankov, V.I., Gunin, P.D., Tsoog, S., Black, C.C., 2000. C4 plants in the vegetation of Mongolia: their natural occurrence and geographical distribution in relation to climate. Oecologia 123, 15–31.
Quade, J., Cerling, T.E., Bowman, J.R., 1989. Development of Asian monsoon revealed by marked ecological shift during the latest Miocene in northern Pakistan. Nature 342, 163–166.
Quade, J., Cater, J.M.L., Ojha, T.P., Adam, J., Harrison, T.M., 1995. Late Miocene environmental change in Nepal and the northern Indian subcontinent: stable isotopic evidence from paleosols. Geological Society of America Bulletin 107, 1381–1397.
Rao, Z.G., Zhu, Z.Y., Jia, G.D., Chen, F.H., Barton, L., Zhang, J.W., Qiang, M.R., 2010. Relationship between climatic conditions and the relative abundance of modern C_3 and C_4 plants in three regions around the North Pacific. Chinese Science Bulletin 55 (18), 1931–1936.
Stauffer, B., Blunier, T., Dallenbach, A., Indermuhle, A., Schwander, J., Stocker, T.F., Tschumi, J., Chappellaz, J., Raynaud, D., Hammer, C.U., Clausen, H.B., 1998. Atmospheric CO_2 concentration and millennial-scale climate change during the last glacial period. Nature 392, 59–62.
Stevens, T., Armitage, S.J., Lu, H.Y., Thomas, D.S.G., 2006. Sedimentation and diagenesis of Chinese loess: implications for the preservation of continuous high-resolution climate records. Geology 34, 849–852.
Sun, J.M., 2000. Origin of eolian sand mobilization during the past 2300 years in the Mu Us Desert, China. Quaternary Research 53, 73–88.
Sun, J.M., Li, S.H., Han, P., 2006. Holocene environmental changes in the central Inner Mongolia, based on single-aliquot-quartz optical dating and multi-proxy study of dune sands. Palaeogeography, Palaeoclimatology, Palaeoecology 233, 51–62.
Vidic, N.J., Montañez, I.P., 2004. Climatically driven glacial–interglacial variations in C_3 and C_4 plant proportions on the Chinese Loess Plateau. Geology 32, 337–340.
Wang, R.Z., 2004. C_4 plants and the relations with desertification in Hunshandake desert grassland. Acta Ecologica Sinica 24, 2225–2229.
Wang, B. (Ed.), 2006. The Asian Monsoon. Paracis publishing Ltd, Chichester, UK. 787 pp.
Wang, T., 2008. Strategic consideration on desert and desertification sciences development in China. Journal of Desert Research 28, 1–7.
Wang, H., Follmer, L.R., 1998. Proxy of monsoon seasonality in carbon isotope from paleosols of the southern Chinese Loess Plateau. Geology 26, 987–990.
Wang, H., Ambrose, S.H., Liu, J.C.-L., Follmer, L.R., 1997. Paleosol stable isotope evidence for early Hominid Occupation of East Asian Temperate environments. Quaternary Research 48, 228–238.
Wang, G.A., Han, J.M., Liu, D.S., 2003. The carbon isotope composition of C-3 herbaceous plants in loess area of northern China. Science in China: Earth Sciences 46, 1069–1076.
Wang, X.M., Zhou, Z.J., Dong, Z.B., 2006. Control of dust emissions by geomorphic conditions, wind environments, and land uses in northern China: an examination based on dust storm frequency from 1960 to 2003. Geomorphology 81, 292–308.
Wang, W., Ma, Y.Z., Feng, Z.D., Meng, H.M., Sang, Y.L., Zhai, X.W., 2009. Vegetation and climate changes during the last 8660 cal. a BP in central Mongolia, based on a high-resolution pollen record from Lake Ugii Nuur. Chinese Science Bulletin 54, 1579–1589.
Wedin, D.A., Tieszen, L.L., Dewey, B., Pastor, J., 1995. Carbon-isotope changes during grass decomposition and soil organic-matter formation. Ecology 76, 1383–1392.
Wen, R.L., Xiao, J.L., Chang, Z.G., Zhai, D.Y., Xu, Q.H., Li, Y.C., Itoh, S., 2010. Holocene precipitation and temperature variations in the East Asian monsoonal margin from pollen data from Hulun Lake in northeastern Inner Mongolia, China. Boreas 39 (2), 262–272.
Wiesenberg, G.L.B., Schwarzbauer, J., Schmidt, M.W.I., Schwark, L., 2004. Source and turnover of organic matter in agricultural soils derived from n-alkane/n-carboxylic acid compositions and C-isotope signatures. Organic Geochemistry 35, 1371–1393.
Wittmer, M., Auerswald, K., Tungalag, R., Bai, Y.F., Schaufele, R., Schnyder, H., 2008. Carbon isotope discrimination of C3 vegetation in Central Asian grassland as related to long-term and short-term precipitation patterns. Biogeosciences 5, 913–924.
Wu, B., Ci, L.J., 2001. Temporal and spatial patterns of landscape in the Mu Us sand land, northern China. Acta Ecologica Sinica 21, 191–196.
Wynn, J.G., Bird, M.I., Wong, V.N.L., 2005. Rayleigh distillation and the depth profile of $^{13}C/^{12}C$ ratios of soil organic carbon soils of disparate texture in Iron Range National Park, Far North Queensland, Australia. Geochimica et Cosmochimica Acta 69, 1961–1973.
Wynn, J.G., Harden, J.W., Fries, T.L., 2006. Stable carbon isotope depth profiles and soil organic carbon dynamics in the lower Mississippi Basin. Geoderma 131, 89–109.
Xiao, J.L., Nakamura, T., Lu, H.Y., Zhang, G.Y., 2002. Holocene climate changes over the desert/loess transition of north-central China. Earth and Planetary Science Letters 197, 11–18.
Xiao, J.L., Xu, Q.H., Nakamura, T., Yang, X.L., Liang, W.D., Inouchi, Y., 2004. Holocene vegetation variation in the Daihai Lake region of north-central China: a direct indication of the Asian monsoon climatic history. Quaternary Science Reviews 23, 1669–1679.
Xu, D.Y., Kang, X.W., Liu, Z.L., Zhuang, D.F., Pan, J.L., 2009. Assessing the relative role of climate change and human activities in sandy desertification of Ordos region, China. Science in China: Earth Science 52 (6), 855–868.
Yang, L.H., Zhou, J., Lai, Z.P., Long, H., Zhang, J.R., 2010. Lateglacial and Holocene dune evolution in the Horqin Dune field of northeastern China based on luminescence dating. Palaeogeography, Palaeoclimatology, Palaeoecology 296, 44–51.
Yin, L.J., Li, M.R., 1997. A study on the geographic distribution and ecology of C4 plants in China—I C4 plant distribution in China and their relation with regional climatic condition. Acta Ecologica Sinica 17 (4), 350–363.
Zhai, D.Y., Xiao, J.L., Zhou, L., Wen, R.L., Chang, Z.G., Wang, X., Jin, X.D., Pang, Q.Q., Itoh, S., 2011. Holocene East Asian monsoon variation inferred from species assemblage and shell chemistry of the ostracodes from Hulun Lake, Inner Mongolia. Quaternary Research 75 (3), 512–522.
Zhang, X.Y., Gong, S.L., Zhao, T.L., Arimoto, R., Wang, Y.Q., Zhou, Z.J., 2003. Sources of Asian dust and role of climate change versus desertification in Asian dust emission. Geophysical Research Letters 30, 2272. doi:10.1029/2003GL018206.
Zhang, Z.H., Zhao, M.X., Lu, H.Y., Faiia, A.M., 2003. Lower temperature as the main cause of C_4 plant declines during the glacial periods on the Chinese Loess Plateau. Earth and Planetary Science Letters 214, 467–481.
Zhang, T.H., Zhao, H.L., Li, S.G., Li, F.R., Shirats, Y., Okhuro, T., Taniyama, I., 2004. A comparison of different measures for stabilising moving sand dunes in the Horqin Sandy Land of Inner Mongolia, China. Journal of Arid Environments 58, 203–214.

Zhang, B.L., Tsunekawa, A., Tsubo, M., 2008. Contributions of sandy lands and stony deserts to long-distance dust emission in China and Mongolia during 2000–2006. Global and Planetary Change 60, 487–504.

Zhao, L.J., Xiao, H.L., Cheng, G.D., Liu, X.H., Yang, Q., Yin, L., Li, C.Z., 2009. Correlation between $\delta^{13}C$ and $\delta^{15}N$ in C_4 and C_3 plants of natural and artificial sand-binding microhabitats in the Tengger Desert of China. Ecological Informatics 5, 177–186.

Zhou, Y.L., Lu, H.Y., Mason, J., Miao, X.D., Swinehart, J., Goble, R., 2008. Optically stimulated luminescence dating of aeolian sand in the Otindag dune field and Holocene climate change. Science in China Series D: Earth Sciences 51, 837–847. doi:10.1007/s11430-008-0057-9.

Zhou, Y.L., Lu, H.Y., Zhang, J.F., Zhou, L.P., Miao, X.D., Mason, J.A., 2009. Luminescence dating of sand–loess sequences and response of Mu Us and Otindag sand fields (north China) to climatic changes. Journal of Quaternary Sciences 24 (4), 336–344.

https://doi.org/10.1016/j.yqres.2012.01.009 Published online by Cambridge University Press